ANALYSIS OF THE INFLUENCE OF THE CRACK PROPAGATION ANGLE IN THE THIN ALUMINUM PLATES UNDER THE EFFECTS OF THE TRACTION EFFORTS

Sofiane CHORFI[1], Brahim NECIB[2]

The analysis of the crack propagation in the industrial plate structures leads to assess their lifetime before their sudden break. In this work, the position of the crack propagation angle around holes in thin aluminum plates under the effects of external applied forces is considered. The hole priming position is defined by a point on the edge of the hole and the inclination angle with respect to the orthonormal axis (X,Y) whose center is the center of the hole. For this case, an analytical multi-scale approach by use of the finite elements method to make a map of the damage before interesting locally on the boot for cracks. The analysis is carried out using the ANSYS code programmer with a parametric design language (APDL). As a result, a calculation strategy is implemented based on the "special quarter-point" finite element method involving the BEM and XFEM approach. The obtained results allowed us to define the crack propagation mode (Mode I, II or III) and to calculate the values of their stress intensity factors corresponding to each mode. The numerical results are compared to the experimental and good results were observed.

Keywords: Plate with hole, Modes, Intensity Factors, Crack length, Angles of propagations, Tensile forces.

1. Introduction

Perforated plates have many practical applications [1-2], especially in mechanics, aeronautics, biomechanics and other structures assembled, by bolts or rivets, etc. Nowadays, the study of the tensile phenomenon on these plates shows a weakening that occurs due to the presence of local stresses or stress concentrations at these holes [3]. It is therefore advisable to avoid, as much as possible, drilling which increases the probability of the presence of cracks [4]. However, since the presence of these factors is inevitable, it is necessary to know the constraint concentration factor associated with each geometry in order to dimension these structures, to avoid their disaster and to increase their lifetime, something that is considered in our problem.

[1]Mechanical Engineering Department, Laboratory of Mechanics, University Frères Mentouri Constantine 1, Algeria. e-mail: sofna25000@yahoo.fr
[2]Mechanical Engineering Department, Laboratory of Mechanics, University Frères Mentouri Constantine 1, Algeria. e-mail: necibbrahim2004@yahoo.fr

During the last decade, the propagation of fissures in thin perforated plates plays an important role in the field of research and engineering in order to avoid the destruction and total cracking of mechanical, aeronautical and civil engineering structures [5]. Sih and Lee studied the theoretical behavior of cracked plates under external loads, the length of cracks under the effect of the critical load; then they showed the forms of the modes related to these plates [6]. Shaw, Huang and Riks studied the behavior of cracked plates under tensile force by the finite element method and examined the effect of crack length [7-8]. They proved the validity of their relations by the finite element method. Brighenti used the numerical method and analytical method to study the phenomenon of the propagation of cracks in perforated plates under external loads [9-11]. He studied the effect of mechanical and geometric variables such as the Poisson's ratio, the boundary conditions, the crack length, and the initiation angle. The results indicated that each of these parameters has a considerable effect on the buckling load. Shariati and al. have done a numerical study of the direction of crack propagation under axial compression loading in elastic-plastic materials by considering some parameters, such as length, crack angle, and boundary condition, imperfection, and characteristics with different materials of the plates [12].On the other hand, Griffith has developed that the presence of these defects in a material could amplify the local stress. The latter can reach a value equal to the tensile strength without increasing the external applied stress. This principle can also be applied to all geometric discontinuities present in a material such as an internal or external crack [13]. In general, the macroscopic direction of propagation of a crack is generally perpendicular to the stress that contributes to the opening of it. This configuration is called the open mode (mode I). Two other propagation modes exist: the plane shear mode (mode II), and the anti-plane shear mode (mode III) [14]. The approach based on the linear mechanics of fracture is in three variables; the applied stress, the toughness K_c that replaces the yield strength that is the size of the defect. There are, however, two alternative approaches to fracture mechanics, one using the concept of critical stress intensity (material toughness) and the other using the energy criterion. These two approaches are equivalent under certain conditions. A number of break-out criteria have been developed by many researchers, for example: criteria of maximum circumferential stresses proposed by Erdogan and Sih [15], the criterion of tension energy density factor presented by Sih [16,17], and the opening of the crack point developed by Sutton and al. [18].

Our work is the continuity of [19] and a contribution to the analysis of the propagation of a crack near the hole in a thin aluminum under external tensile stress. Two main factors were considered: the position of the initiation of the crack and the angle of propagation of the crack. The priming position of the hole is defined by a point on the periphery of the hole and the inclination angle that is

relative to the orthonormal axis (X, Y) whose origin is the center of the hole. Two positions are chosen: initiation on the abscissa axis X, corresponding to the 0 ° angle and initiation at 45°. For each of the positions, the crack propagation is simulated in 4 directions: 0°, 30°, 60°, and 90°.The objective is such that for each of the starting points of the crack, to study the influence of the variation of the angle of propagation. The study carried out numerically using APDL ANSYS (for the EF and BEM method) and ABQUS for the XFEM method [20-25]. The numerical results obtained are compared to the experimental results.

2. Mathematical model

For the evaluation of the stress intensity factor, consider in our case, an isotropic thin plate pierced with a circular hole is considered in order to determine the stresses and deformations around the holes. The latter can be obtained from the stress concentration factor K_t [19] which is given by:

$$K_t = \frac{\sigma_{\max}}{\sigma_N} = \frac{\varepsilon_{\max}}{\varepsilon_N} \tag{1}$$

Where σ_{max} and ε_{max} are respectively local maximal stress and local maximal strain, while σ_N and ε_N are the nominal stress and the nominal strain. In the case of constraint singularity, the computation of the stress intensity factor "SIF" is also complicated because it is function of the position along the crack front, crack size as well as its shape, type of loading and geometry of the structure.

In this study, the special finite elements analysis called the quarter-point proposed by Barsoum [26]. It has singular elements which represent displacements and pulls, which are used to obtain a better approximation of the field around the crack's point front (Fig.1) where the mid side node of the element connected to the point of the front moved to 1/4 of the length of this element. "SIF" solutions can be calculated using a kinematic extrapolation technique of displacement [27]; this implies the correlation of the elements boundary displacements on the surface of crack "Boundary Element Method" with those of the theoretical values of the Irwin formula. The results of "SIF" are calculated at two locations far from the crack tip. The extrapolation technique is illustrated in the diagram represented in Fig.1 .

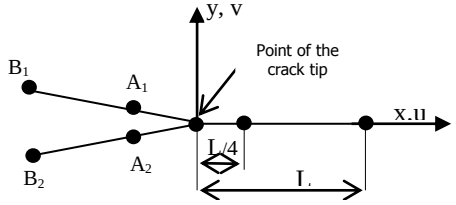

Fig.1. Description of the extrapolation technique [24]

$$K_I = \frac{E_{tip}}{3(1+\upsilon_{tip})(1+k_{tip})}\sqrt{\frac{2\pi}{L}}\left[4(V_{A_1}-V_{A_2})-\frac{(V_{B_1}-V_{B_2})}{2}\right]$$
$$K_{II} = \frac{E_{tip}}{3(1+\upsilon_{tip})(1+k_{tip})}\sqrt{\frac{2\pi}{L}}\left[4(u_{A_1}-u_{A_2})-\frac{(u_{B_1}-u_{B_2})}{2}\right] \quad (2)$$

where: E_{tip} and υ_{tip}; are Young's modulus and Poison Coef. In the point of the crack tip: u_n, v_n(n=1,2) are the nodal displacements in the nodes A_1, A_2, B_1, B_2 respectively in the x, y directions. The length element of the singular side is L.

$$k_{tiip} = \frac{(3-\upsilon_{tip})}{(1+\upsilon_{tip})} \qquad \text{PLANE STRESS}$$
$$k_{tiip} = \frac{(3-\upsilon_{tip})}{(1+\upsilon_{tip})} \qquad \text{PLANE STRAIN} \quad (3)$$

The stress intensity factors according to Richard [28] give KI and KII solutions for a central crack, flat and normal to the lateral faces. The stress intensity factors for different angles of initial cracking orientation of XFEM are given by the following expressions [29]:

$$K_I = \sigma\sqrt{\pi a}\,\frac{\cos\alpha}{\left(1-\frac{a}{W}\right)}\sqrt{\frac{0{,}26+2{,}65\left(\frac{a}{W-a}\right)}{1+0{,}55\left(\frac{a}{W-a}\right)+0{,}08\left(\frac{a}{W-a}\right)^2}}$$
$$K_{II} = \sigma\sqrt{\pi a}\,\frac{\sin\alpha}{\left(1-\frac{a}{W}\right)}\sqrt{\frac{-0{,}23+1{,}4\left(\frac{a}{W-a}\right)}{1+0{,}67\left(\frac{a}{W-a}\right)+2{,}08\left(\frac{a}{W-a}\right)^2}} \quad (4)$$

3. Crack modeling strategy

In this article, the APDL code has been used to highlight the program to simulate the propagation of cracks by making the increment i+1 of the position either the pitch or the angle of propagation of the perforated plate's crack (Fig.2).Thus, one can introduce the formulas of the crack stress intensity factor in each orientation or position of the perforated plate. The figure illustrates the flowchart of the prepared APDL code based on the combination of the BEM and XFEM approach.

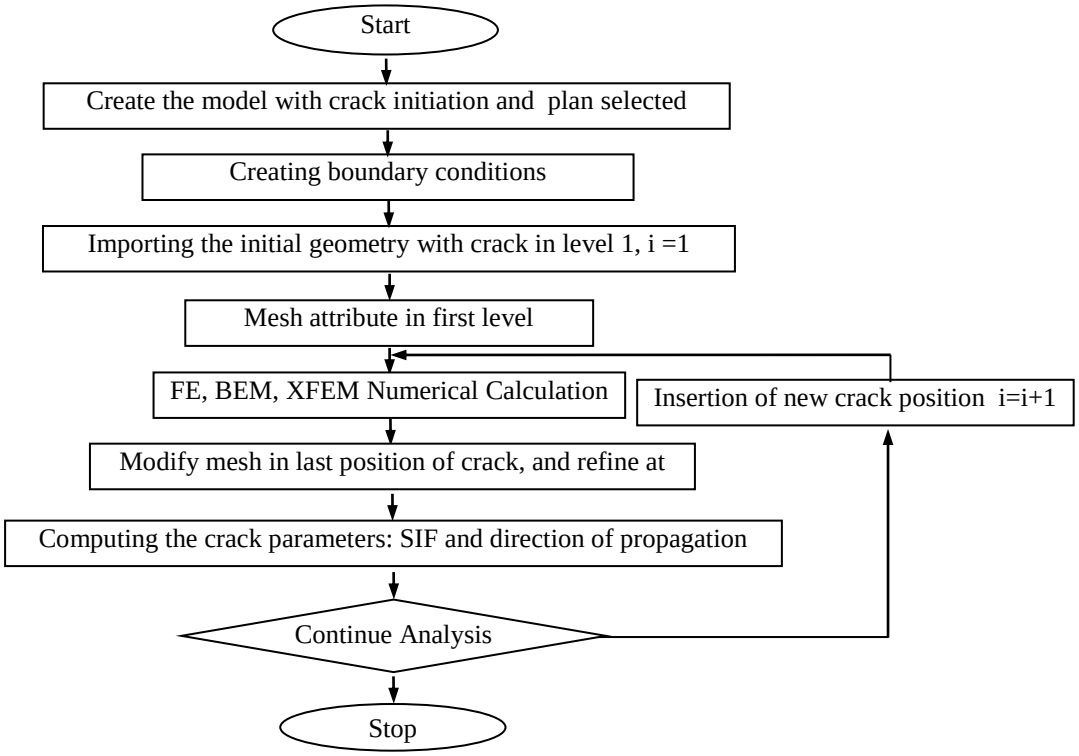

Fig.2. Flow chart of the cracks propagation simulation in the plate perforated

4.Numerical analysis of crack initiation

4.1. Material of study

Aluminum 7075-T6 present a very high strength material used for highly stressed structural parts (Aircraft fittings, gears and shafts, aerospace and defense applications). The T7351 temper offers improved stress-corrosion cracking resistance. Calculations are made based on the properties of the 7075-T6 aluminum plate material (SS), see Table 1:

Table 1

Material Characteristic

Young's Modulus "E"	Poisson's ratio *v*	Tensile Strength.	Mass density	Elasticity limit
$7{,}19999 * 10^9$	0,3	$5{,}7 * 10^8$ N/m²	2810 Kg/m^3	$5{,}07 * 10^8$ N/m²

The chemical composition is reported in Table 2

Table 2

Chemical composition

Component	*AL*	*Cr*	*Cu*	*Fe*	*Mg*	*Mn*	*Si*	*Ti*	*Zn*
Wt. %	87.1 - 91.4	0.18 - 0.28	1.2 - 2	≤ 0.5	2.1 - 2.9	≤ 0.3	≤ 0.4	≤ 0.2	5.1 - 6.1

4.2. Geometry of the plate

The experiments were carried out in an electronic traction test machine (100KN) mechanical testing machine shown in Fig.3a., Interfaced to a computer for machine control and data acquisition. All tests were conducted in air and at room temperature. For the numerical method we consider a thin perforated aluminum plate, the thickness, width and length of which are 3mm, 35mm and 100mm, respectively, and a 10mm diameter hole. In our study, only one-quarter of the plate is used to save work time (see Fig.3b).

Fig.3a. electronic traction test machine 100KN

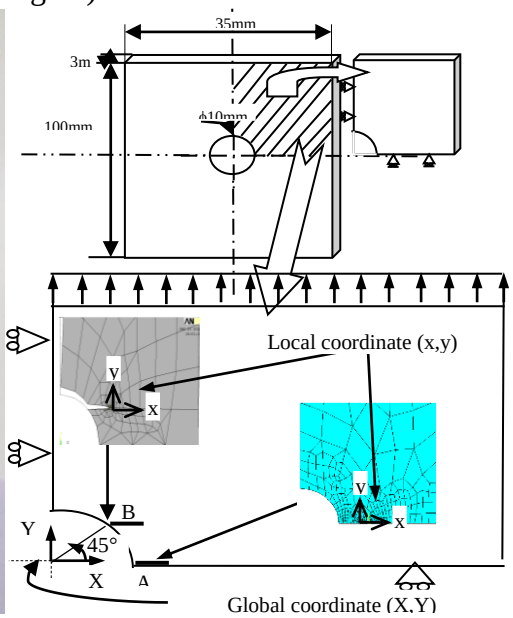

Fig.3b. Geometry of the plate in axial tension including a crack A, B

In this case, we assume that the tensile load is applied along the Y axis and that the crack is initiated in the points A, B of the edge of the hole at an angle of 0°, 45° respectively relative to the global origin XY. Then, we analyze the stress variation and the stress intensity factor according to the length of the cracks and the different angles of orientation.

The origin of the global coordinate system (XY) is in the center of the hole. Under the pulling effect the ends of the plate move only along the perpendicular axes. This indicates the appropriate travel conditions to use as shown below. We will use numerical methods to determine the stress in the maximum horizontal patch of the plate and compare the calculated results with the maximum value that could be calculated using the tabulated values [30-31] (see Fig.14).

4.2. Mesh effect on the maximum stress applied to the plate

A refined mesh is well constructed which consists of quadrangular elements near the crack's tip to visualize clearly the propagation of the crack. According to the geometry of the plate, the concentration factor of the theoretical constraints is Kt = 2.17 [19].

If we consider the area of the transverse part St= 0.002 mm², and the excitation pressure P = 1 Pa, the maximum stress is then σ_{max} = 4.34 Pa [19]. In addition, the values of the maximum stress are calculated numerically using two types of meshes. The first less refined (Fig.4a) gave a value of 4.59 Pa, with an error of 5.8%; the second, more refined (Fig.4b), a value of 4.38 Pa, with an error of 1%. In conclusion, the more the mesh is refined, the more the results of the maximum stress converge to the exact values.

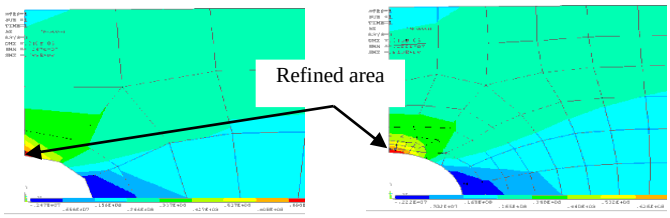

(a) Normal mesh (b) Fine mesh

Fig.4. The stress σ_{max} for different meshes

4.3. Effect of the crack initiation position and angle

On the basis of the numerical analysis carried out, the equivalent stress of Von Misses was obtained for the various position (A, B) and angle of initiation of the crack (0°, 30°, 45°, 60°, 90°) , are presented on Fig. 9. The maximum value recorded during this simulation is in the singularity of stress in the front of the crack around this point in observes a plastic zone which supports the propagation of the crack.

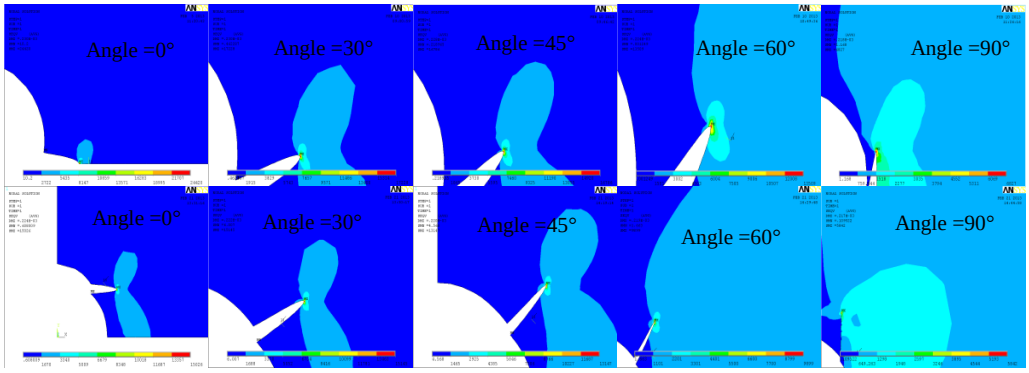

Fig. 5. Von misses Stress distribution field for the different position and angle crack initiation

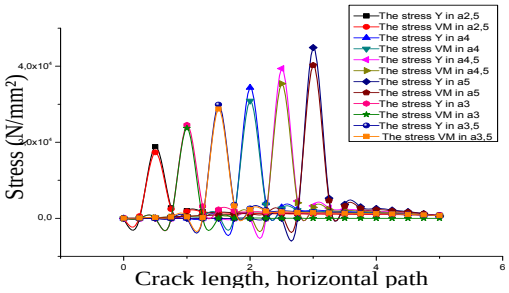

Fig.6. Stress distribution according to the horizontal patch for crack at 0 ° (point A)

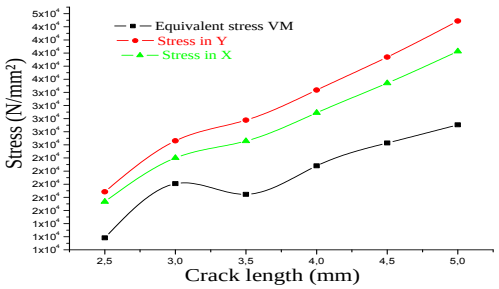

Fig.7. Variation of stresses as a function of crack length at 0° (point A)

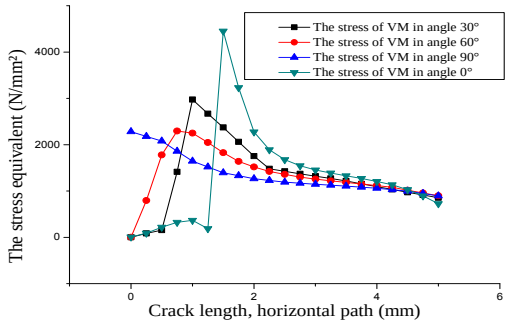

Fig.8. Variation of the stresses according to the angle of initiation of the points A

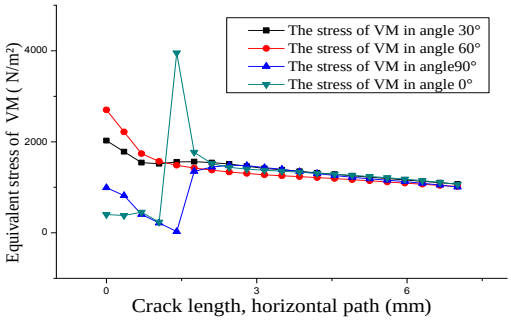

Fig.9. Variation of the stresses according to the angle of initiation of point B

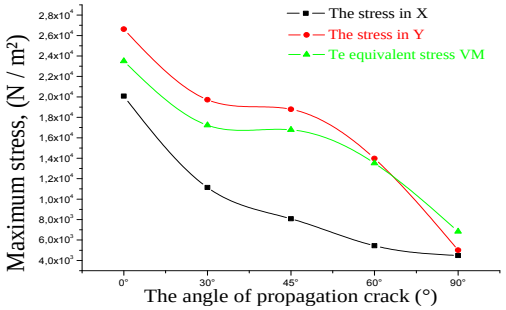

Fig.10. Variation of the stress according to the angle of propagation crack (point A at 0°)

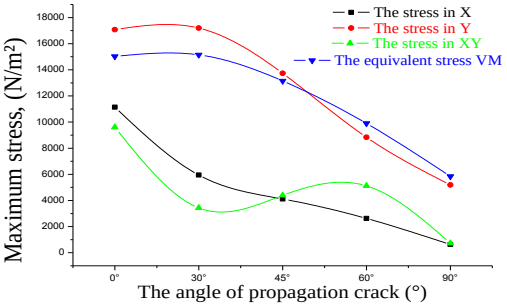

Fig.11. Variation of the stress according to the angle of propagation crack (point B at 45°).

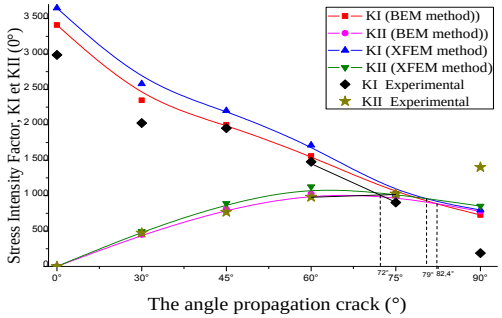

Fig.12.Variation of the stress intensity according to the angle of propagation crack (A)

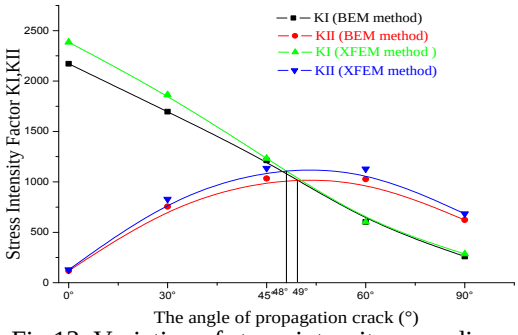

Fig.13. Variation of stress intensity according to the angle of propagation crack (B at 45°).

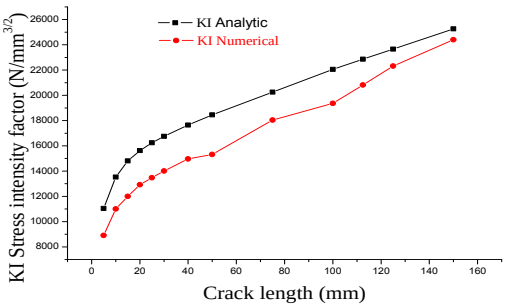

Fig.14. Variation of stress intensity factor according to the crack length (A at 0°)

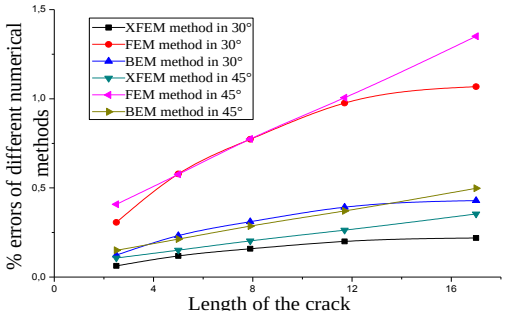

Fig.15. Errors of different numerical methods according to the crack length in angles 30°, 45°

5.Discussion of the results

The transformation of Cartesian global coordinates (OXY) into local coordinates for crack point tracking and crack propagation direction helps to find the stresses and stress intensity factors in each step and crack orientation. There are several crack initiation points at the edge of the plate hole. In this study, we consider two emergent points of the hole, the position of the first crack initiation point at 0° (point A), and the second point at 45° (point B).

From Fig.6 and Fig.7, an increase in stress as a function of crack length has been observed, whereas there is a decrease in stress as a function of the angle of propagation (Figs. 8, 9, 10 and 11).

The stress intensity factor K increases as a function of the crack length for both analytical and numerical approaches. The SIF study, characterizing the crack, was performed using two numerical methods, XFEM and BEM, represented in table 2.In this work, by transforming the Cartesian global coordinates (OXY) into local coordinates while following the crack point and propagation direction find the constraints and stress intensities factors in each step and orientation of cracking. In Fig.6 and fig.7, a stress increase following the horizontal patch of the crack length (at 0°), where a singularity of stress is observed at each crack front. While this is the constraint for angle 30°, 60°, and 90° (Fig.8, 9).From FIG.14, the

stress intensity factor (K) increases as a function of crack length for both analytical and numerical approach. In Fig.10,11 there is a decrease in stress by varying the initiation angle.

Two cases were considered in the analysis of cracks emerging from thin plate holes: the crack initiation position and angle, and the crack propagation length. From the following tables, we observe the SIF factors that characterize the crack according to two numerical methods XFEM and BEM.

Table 3

The stress intensity factor according BEM method and XFEM method

Position of crack initiation		**According BEM method** Angle of propagation of the crack.					**According XFEM method** Angle of propagation of the crack.				
		0°	30°	45°	60°	90°	0°	30°	45°	60°	90°
0°	KI	3409.8	2347.8	2001.6	1558.8	725.47	3676.2	2580.0	2199.6	1712.9	797.22
	KII	0	449.26	808.97	1025.5	775.97	0	493.69	888.98	1126.9	852.72
45°	KI	2171.6	1695.9	1212.6	602.53	259.26	2386.3	1863.7	1332.6	662.13	284.90
	KII	117.21	754.54	1033.1	1027.5	622.54	128.80	829.16	1135.3	1129.1	684.11

According to Fig.13, for the experimental approach and the two numerical approaches; a crack initiated at 0°, the stress intensity factor KI takes its maximum value in the direction of propagation of 0° then it decreases gradually until it reaches its minimum value at the 90° angle. While the SIF KII takes the value zero at the 0° angle, then it increases to approach the maximum value at 90°. The tensile and shear stresses around the tip of the pre-crack are equivalent to the angle 72° in the experimental results, and equal to 78°, 82.4° respectively in numerical results of the method XFEM and BEM. Up to this value tensile stresses dominates and above it shear stresses dominates.

Whereas for a crack initiated at 45° (Fig. 14), gives rise to two failure modes (mode I and mode II), also called mixed modes. By varying the propagation angle, the SIF KI at the 0° angle is of maximum value, then it gradually decreases to the 90° angle, while the SIF KII at 0° is of minimum value not zero; it then increases to the 90° angle and KII becomes greater than KI. The tensile and shear stresses around the point of the pre-crack are equal to the angle 48°, 49° respectively in numerical results of the method XFEM and BEM, Table 3.

The evolution of the error percentages of the numerical solutions studied (Fig. 15) is calculated with respect to an exact model solution [32].An increase in errors is observed as a function of the length of the crack, and the percentage of errors is considerable for the finite element method compared to the XFEM and BEM methods.

6. Conclusion

The propagation of a crack is possible in the holes of the plates, in the presence of a stress concentration weakening the structure. This concentration tends towards a crack initiation that cannot be predicted and a difficult to model. It is therefore necessary to create the boot of the crack manually. Indeed, the numerical study carried out on the influence of the position, the initiation angle around the hole of the aluminum thin plate and on the behavior under the effect of a simple tensile load.

Considering the singular quarter-point element of traction, on each side of the crack, we can deduce that it is necessary to choose the quarter point element and the refinement of the mesh for a better convergence towards the exact solution.

We note a proportionality between the crack propagation and the stress intensity factor. The XFEM and BEM methods, according to an approximation singularity, showed low error levels compared to the classical finite element methods, which showed higher error levels. The first XFEM makes it possible to calculate a propagation with a single mesh, while the second BEM requires discretization at the boundary of the object. For the good investigation, it is imperative to know the starting point of the crack and its angle of propagation which is responsible for the stresses type (tensile or shear) around the point of the pre-crack, and their mode (pure or mixed mode).

R E F E R E N C E S

[1]. *J. Rezaeepazhand, M. Jafari,* "Stress concentration in metallic plates with special shaped cutout", International Journal of Mechanical Sciences, vol. 52, no. 1, 2010, pp. 96-102.

[2]. *P.M.G.P. Moreira, S. D. Pastrama and P.M.S.T. de Castro*, " Comparative Three Dimensional Fracture Analyses of Cracked Plates", U.P.B. Sci. Bull., Series D, vol.69, no. 1 69, 2007, pp.43-58.

[3]. *B.C.L. Vanam, M. Aajyalakshmi and R. Inala*, "Static analysis of an isotropic rectangular plate using finite element analysis (FEA) ", Journal of Mechanical Engineering Research., vol. 4, no. 4, 2012, pp. 48-162.

[4]. *Flora SALGADO GONCALVES*, Caractérisation expérimentale et modélisation des interactions entre fissures et perçages multiples à haute température en élasto-plasticité généralisée ou confinée, Thèse de doctorat, l'École nationale supérieure des mines de Paris2013.

[5]. *L. Khammar,* "Thermo mechanical modeling of cracked brake disc" journal U.P.B. Sci. Bull., Series D, Vol. 80, Iss.1,2018.

[6]. *GC. Sih and YD. Lee*, "Tensile and compressive buckling of plates weakened by cracks", *Theoretical and Applied Fracture Mechanics*, Vol. 6, No. 2, pp. 129-138, (1986).

[7]. *D. Shaw and Y. H. Huang,* "Buckling behavior of a central cracked thin plate under tension", *Engineering Fracture Mechanics,* Vol. 35, No. 6, pp. 1019- 1027, (1990).

[8]. *E. Riks, CC. Rankin and FA. Bargon,* "Buckling behavior of a central crack in a plate under tension", *Engineering Fracture Mechanics,* Vol. 43, No. 4, pp. 529-548, (1992).

[9]. *R. Brighenti*, "Numerical buckling analysis of compressed or tensioned cracked thin plates", *Engineering Structure,* Vol. 27, No. 2, pp. 265-276, (2005).

[10]. *R. Brighenti*, "Buckling of cracked thin plates under tension or compression", *Thin-Walled*

Structure, Vol. 43, No. 2, pp. 209-224, (2005).
[11]. *R. Brighenti*, "Buckling sensitivity analysis of cracked thin plates under membrane tension or compression loading", *Nuclear Engineering and Design*, Vol. 239, No. 6, pp. 965-980, (2009).
[12]. *M. Shariati and A. M. Majd Sabetib*, "A Numerical and Experimental study; Buckling and post-buckling of cracked plates under axial compression load", *Journal of Computational and Applied research in Mechanical Engineering*, Vol. 4, No. 1, pp. 43-54, Autumn 2014.
[13]. *J.M. Dorlot, J.-P. Bailon, et J. Masounave*, "Des matériaux" Editions de l'école Polytechnique de Montréal (1986), 467 p.
[14]. *H. Proudhon* " Identification des Mécanismes de Fissuration dans un Alliage d'aluminium Sollicité en Fretting et en Fatigue" Thèse de Doctorat, Génie de matériaux de Lyon 2005.
[15]. *F. Erdogan and GC. Sih*, On the crack extension in plates under plane loading and transverse shear. Journal of Basic Engineering 85 (1963)519-27.
[16]. *GC. Sih*, A special theory of crack propagation. Leyden: Noordhoff International Publishing; Mechanics of fracture 1 (1973).
[17]. *GC. Sih*, Strain energy-density factor applied to mixed mode crack problem. International Journal of fracture 10, 3 (1974) 305-21.
[18]. *M. A. Sutton, X. Deng, F. Ma F, Jr JC Newman*, M. James. Development and application of a crack tip opening displacement- Based mixed mode fracture criterion. International Journal of solids and structures 37 (2000) 3591-618.
[19]. *S. Chorfi, B. Necib*. Crack propagation analysis around the holes in the plates under the effect of external stresses using the finite element model**,** ESIS Summer School, ECF21, June 20-24, 2016.
[20]. *R .Branco, FV. Antunes, JD. Costa*, A review on 3D-FE adaptive remeshing techniques for crack growth modeling. Engineering Fracture Mechanics. 2015;141:170-95.
[21]. *E. Santana, A. Portela*, Dual boundary element analysis of fatigue crack growth, interaction and linkup. Engineering Analysis with Boundary Elements. 2016;64:176-95.
[22]. *Q. Zeng, Z. Liu, D. Xu, H. Wang, Z. Zhuang*, Modeling arbitrary crack propagation in coupled shell/solid structures with X-FEM. International Journal for Numerical Methods in Engineering. 2016;106(12):1018-40.
[23]. *T. Belytschko, R. Gracie, G. Ventura*, A review of extended/generalized finite element methods for material modeling. Modeling and Simulation in Materials Science and Engineering. 2009;17(4):043001.
[24]. *Abaqus* Tutorial, on Static stress/displacement analyses, modeling a plate with a crack,*2014*
[25]. *ANSYS*, Programmer's Manual for Mechanical APDL, Release 15.0 , 2014.
[26]. *R. S. Barsoum*, On the use of isoparametric finite element in linear fracture mechanics, International Journal for Numerical Methods in Engineering. 10 (1974) pp. 25-37
[27]. *RyojiYuuki and Sang-bong Cho*, Efficient boundary element analysis of stress intensity factors for interface cracks in dissimilar materials, Engin. Fract. Mechcs. 1989, Vol. 34, No. I, pp. 179-188.
[28]. *HA. Richard*, Bruchvorhersagen*bei*¨berlagerter normal- und schubbeanspruchung von risen VDI Forschungsheft631. Dusseldorf: VDI-Verlag; 1985. p. 1-60.
[29]. *L.P. Borrego, F.V. Antunes*. "Mixed-mode fatigue crack growth behavior in aluminum alloy", International Journal of Fatigue 28(2006) 618-626.
[30]. *K.L Lawrence*, ANSYS Tutorial, Release 7.0. Schroff Development Corporation (SDC) Publications, *2006*.
[31]. *T.L Anderson*, Fracture Mechanics Fundamentals and Applications, 3rd Edition: CRC press, Taylor & Francis Group, 6000 Broken Sound Parkway NW, Suite 300, Boca Raton, FL 33487-2742, *2005*.
[32]. *M. K. Kassir and G. C. Sih*, Three-dimensional stresses around elliptical cracks in transversely isotropy solids, Engin. Fract. Mechcs. 1968, Vol.1, pp. 327-345..